SPECIAL ISSUE ARTICLE

JOR *Spine* OPEN ACCESS

Development of a standardized histopathology scoring system for intervertebral disc degeneration in rat models: An initiative of the ORS spine section

Alon Lai[1] | Jennifer Gansau[1] | Sarah E. Gullbrand[2] | James Crowley[3] |
Carla Cunha[4] | Stefan Dudli[5] | Julie B. Engiles[6] | Marion Fusellier[7] |
Raquel M. Goncalves[4,8] | Daisuke Nakashima[9] | Jeffrey Okewunmi[1] |
Matthew Pelletier[3] | Steven M. Presciutti[10] | Jordy Schol[11] |
Yoshiki Takeoka[12] | Sidong Yang[13] | Takashi Yurube[14] | Yejia Zhang[2] |
James C. Iatridis[1]

[1]Leni and Peter W. May Department of Orthopaedics, Icahn School of Medicine at Mount Sinai, New York, New York

[2]McKay Orthopaedic Research Laboratory, Department of Orthopaedic Surgery Perelman School of Medicine, University of Pennsylvania, Philadelphia, Pennsylvania

[3]Surgical and Orthopaedic Research Laboratories, Prince of Wales Clinical School, University of New South Wales, Sydney, Australia

[4]i3S-Instituto de Investigação e InovaçãoemSaúde, Universidade do Porto, Porto, Portugal

[5]University Clinic of Rheumatology, Center of Experimental Rheumatology, Balgrist University Hospital, University of Zurich, Zurich, Switzerland

[6]Department of Pathobiology, New Bolton Center, School of Veterinary Medicine, University of Pennsylvania, Kennett Square, Pennsylvania

[7]Regenerative Medicine and Skeleton, Inserm, UMR 1229, RMeS, Université de Nantes, ONIRIS, Nantes Cedex, France

[8]Instituto de CiênciasBiomédicas Abel Salazar, Universidade do Porto, Porto, Portugal

[9]Department of Orthopaedic Surgery, Keio University School of Medicine, Tokyo, Japan

[10]Department of Orthopaedic Surgery, Emory University, Atlanta, Georgia

[11]Department of Orthopaedic Surgery, Surgical Science, Tokai University School of Medicine, Isehara, Japan

[12]Department of Orthopaedic Surgery, Brigham and Women's Hospital, Boston, Massachusetts

[13]Department of Spinal Surgery, The Third Hospital of Hebei Medical University, Shijiazhuang, China

[14]Department of Orthopaedic Surgery, Kobe University Graduate School of Medicine, Kobe, Japan

Correspondence
James C. Iatridis, Leni and Peter W. May Department of Orthopaedics, One Gustave Levy Place, Box 1188, Icahn School of Medicine at Mount Sinai, New York, NY 10029, USA.
Email: james.iatridis@mssm.edu

Funding information
National Institute of Arthritis and Musculoskeletal and Skin Diseases of the National Institutes of Health, Grant/Award Number: R01AR057397

Abstract

Background: Rats are a widely accepted preclinical model for evaluating intervertebral disc (IVD) degeneration and regeneration. IVD morphology is commonly assessed using histology, which forms the foundation for quantifying the state of IVD degeneration. IVD degeneration severity is evaluated using different grading systems that focus on distinct degenerative features. A standard grading system would facilitate more accurate comparison across laboratories and more robust comparisons of different models and interventions.

Aims: This study aimed to develop a histology grading system to quantify IVD degeneration for different rat models.

Materials & Methods: This study involved a literature review, a survey of experts in the field, and a validation study using 25 slides that were scored by 15 graders from different international institutes to determine inter- and intra-rater reliability.

Results: A new IVD degeneration grading system was established and it consists of eight significant degenerative features, including nucleus pulposus (NP) shape, NP area, NP cell number, NP cell morphology, annulus fibrosus (AF) lamellar organization, AF tears/fissures/disruptions, NP-AF border appearance, as well as endplate disruptions/microfractures and osteophyte/ossification. The validation study indicated this system was easily adopted, and able to discern different severities of degenerative changes from different rat IVD degeneration models with high reproducibility for both experienced and inexperienced graders. In addition, a widely-accepted protocol for histological preparation of rat IVD samples based on the survey findings include paraffin embedding, sagittal orientation, section thickness < 10 μm, and staining using H&E and/or SO/FG to facilitate comparison across laboratories.

Conclusion: The proposed histological preparation protocol and grading system provide a platform for more precise comparisons and more robust evaluation of rat IVD degeneration models and interventions across laboratories.

KEYWORDS

histology, histology grading scale, histopathology, intervertebral disc degeneration, intervertebral disc regeneration, rat model

1 | INTRODUCTION

The intervertebral disc (IVD) is the fibrocartilaginous tissue lying between two vertebral bodies that transmits loading along the spine. The IVD separates the spine into small motion segments (vertebra-IVD-vertebra) to provide flexibility and to protect the spinal cord and surrounding tissues by preventing excessive segmentational motion. A healthy IVD is characterized by a hydrated and proteoglycan-rich nucleus pulposus (NP) at the center of the IVD, and a highly organized collagen-rich annulus fibrosus (AF) ring surrounding the NP in concentric lamellae. The IVD is surrounded on superior and inferior surfaces via thin cartilaginous endplates (CEPs), which regulate nutrient and metabolic exchange for the IVD. Degenerative changes in the IVD tissue significantly affect its structure and composition, and can lead to abnormal IVD function.[1]

Understanding pathophysiology of IVD degeneration and investigating therapeutic interventions to slow down the degenerative process or to regenerate damaged IVDs are essential for improving spinal health and reducing pain and disability from IVD degeneration. Human IVD tissues are most relevant to human health, but are limited to surgical or postmortem specimens which are limited in number and have high genetic variability and differences in age, body size, activity level, and spine loading history. Animal models can minimize these sources of variation and are commonly adopted to study IVD degeneration and regeneration, enable collection of multiple tissues across different ages and disease states, and also enable studies on safety, efficacy, and mechanisms of therapeutic interventions for IVD degeneration. Rats

have been frequently used for decades to study IVD degenerative changes since they are relatively inexpensive compared with large animals. Both rat lumbar and coccygeal IVDs consist of proteoglycan-rich NP, collagen-rich AF and CEPs (Figure 1),[2-5] which are structurally and biochemically similar to human IVDs. Despite being relatively small subjects, rats can still be used for multiple surgical procedures, including annular puncture, and intradiscal injection.[2-11] Rat IVD degeneration models are particularly important since they enable the measurement of pain-associated behaviors due to well-established behavioral assays.[7,12-17] Moreover, the rat model is a useful preclinical tool for determining the efficacies and mechanisms of experimental therapeutic interventions for both IVD degeneration and discogenic pain.

A reliable method to generate IVD defects is essential in order to investigate pathophysiology and therapeutic interventions for IVD degeneration. Different strategies have been used to induce degenerative changes in rats, including the naturally occurring disc degeneration in aged animals,[18-21] surgery injury,[4,5,7,12,13,22-27] and mechanical loading.[28-40] The process of naturally induced IVD degeneration is slow and the severity of tissue damage can vary between animals. Surgical injury is widely adopted for inducing degeneration in lumbar IVD, while both surgical and mechanical approaches are commonly used for coccygeal IVDs. With the different strategies for inducing IVD degeneration as well as the development of different therapeutic interventions for IVD regeneration, there remains the need to objectively and reliably quantify the severity of IVD degeneration.

A variety of histological grading systems are available for semi-quantitatively assessing the severity of degeneration in rat IVDs.[6,41-45]

FIGURE 1 A non-degenerated healthy rat IVD with safranin-O/Fast-green/Hematoxylin staining. NP, nucleus pulposus; iAF, inner annulus fibrosus; oAF, outer annulus fibrosus; EP, endplate; and GP, growth plate
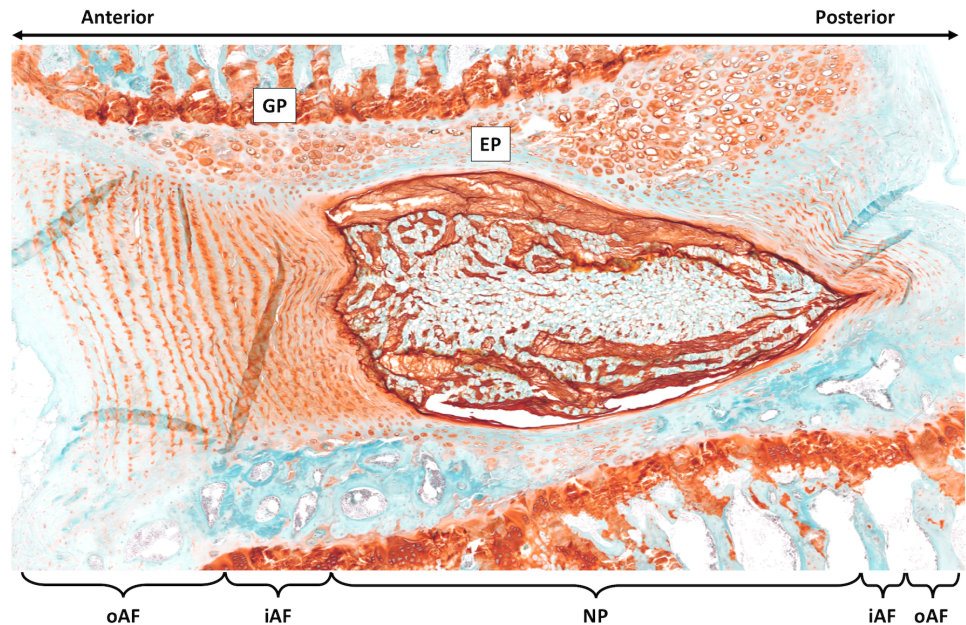
Different subcategories, such as NP morphology, NP cellularity, and NP-AF boundary, were established and scored according to their features of degenerative changes. However, these grading systems are inconsistent with specific subcategories and scoring criteria. Moreover, different studies have different approaches for histological assessment, including the type of staining, thickness of section and specimen orientation, which may also affect the scoring criteria of the grading system.

The overall objective of this study was to establish a standardized and reliable histology grading system which could be used to quantify IVD degeneration in different rat models. Three aims were defined as: (a) to perform a literature review study to identify the most commonly adopted subcategories and features for histological assessments of rat IVD degeneration, (b) to complete a survey study to collect information and feedback from researchers and histology experts about the importance and priority of the histological assessment subcategories and features as identified in Aim 1, and finally (c) to develop a new or modify an existing semi-quantitative rat IVD degeneration grading scheme with subsequent verification using inter- and intra-rater reliability tests for a series of lumbar and coccygeal IVDs histological sections from different degeneration models. This paper also assessed survey results and discussions with the focus group to make recommendations to standardize the protocols for preparing rat IVD histology, including specimen orientation and type of staining, in order to minimize the histology variation that might influence the grading results.

2 | MATERIALS AND METHODS

2.1 | Aim 1: Literature review study

A comprehensive literature search was performed using PubMed through January 16, 2020, with the use of the following keywords: "rat model" AND "intervertebral" AND "degeneration" OR
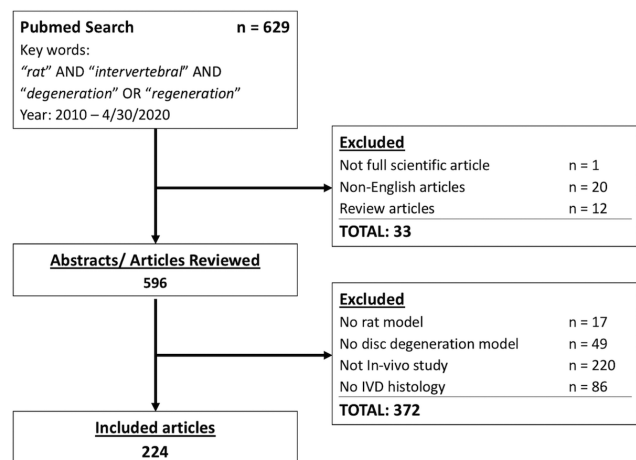
FIGURE 2 Flowchart summarizing the literature review and exclusion criteria. A total of 629 articles were initially identified according to the selected keywords, and 224 articles were finally included for full paper reviewing. IVD, intervertebral disc

"regeneration" (Figure 2). The search was limited to English written articles with all non-English papers being excluded. Studies that involve in vitro cell culture, ex vivo organ culture, computational models, herniation models, and whole (or partial) IVD replacement, as well as review papers or research studies without histological analysis, were beyond the scope of this review and thus excluded. In other words, this literature study focused on the research papers covering IVD degeneration and/or regeneration using in vivo rat models with IVD histology (as one of the outcome measures) to evaluate the severity of degeneration as well as the efficacy of therapeutic interventions.

Full texts of the included studies were retrieved and data was collected for spine levels, IVD specimen orientation, thickness of section,

type(s) of staining being used, if IVD degeneration severity was evaluated, and which histology grading system(s) was (were) used. Lastly, additional category(ies) of outcome measures that were used to assess IVD degeneration were extracted from the included papers (Figure 2).

2.2 | Aim 2: Survey study

Based on the results from the literature review study, a list of widely adopted histological grading systems as well as commonly used IVD morphological categories and degenerative features for scoring the severity of rat IVD degeneration were identified. A survey was created in Google forms to collect information from spine researchers (active members of the Orthopedic Research Society [ORS] Spine section and corresponding authors as identified from the literature review) with respect to their opinion about: (a) which morphological categories and degenerative features should be included in a standardized scoring system, (b) the number of points should be used for each category in the scoring system, as well as (c) the number of raters should be involved. Moreover, this survey also collected information from respondents about their current practices for histologic processing of rat IVDs, including specimen embedding media, specimen orientation, section thickness, and preferred type(s) of staining. The distribution and collection of the survey was deemed exempt research by the Corporal Michael J. Crescenz Veterans Affairs (VA) Medical Center institutional review board (IRB).

2.3 | Aim 3: Validation study

Based on the results of the literature review and survey outcomes as well as the feedback from the discussion of the focus group, a list of morphological categories and degenerative features for IVD degeneration were identified, and were used for the development of a proposed grading system to quantify different morphological characteristics for rat lumbar and coccygeal IVDs. This grading scheme consisted of seven categories (including NP morphology, NP cellularity, NP-AF border, AF morphology, AF cellularity, CEP as well as intradiscal proteoglycan), and a total of 10 IVD degenerative features (Table 1). Each category consisted of one degenerative feature, except for NP morphology, NP cellularity and AF morphology, which were considered as more important morphological characteristics for IVD degeneration and consisted of two features for each category (Table 1). Each feature received a score between 0 and 2 with score 0 for normal morphology and score 2 for characteristic of severe degeneration; therefore, the overall degenerative score was between 0 and 20.

For inter- and intra-rater reliability tests, histological images of rat lumbar and coccygeal IVDs were collected from the respondents of the survey study in Aim 2. A total of 25 slides from eight research groups were selected, blinded, and then scored by 15 graders from different institutes with different experiences for rat IVD histological analysis. Both non-degenerated and degenerated IVDs with varying severity from rat lumbar and coccygeal spines at different ages were included, while the IVD degenerations were induced in response to annular injury, nucleotomy, or mechanical compression. All graders were asked to self-classify as "experienced" (having ≥2 years of experience with rat histopathology grading) or "inexperienced" (<2 years of experience), and they scored the images twice with at least 1 week in between scoring sessions to determine intra-rater reliability. Intra- and inter-rater reliability for each scoring category as well as total score, were determined by calculating intraclass correlation coefficients (ICC) in R (https://www.r-project.org/).

3 | RESULTS

3.1 | Aim 1: Literature review

Based on the keywords and inclusion criteria, a total of 224 studies were reviewed and found suitable for the evaluation of histological analysis methods and degeneration grading systems for rat IVDs in this review (Figure 2). Not all studies included information about each criterion investigated or used, hence there were differences in total numbers for each category. In terms of spine level, the caudal spine was the most commonly used region for studying IVD degeneration (66.7% of all reviewed papers), followed by lumbar and cervical spines (29.8% and 3.6%, respectively) (Figure 3A). Among the three commonly used specimen orientations (sagittal, coronal, and transverse), sagittal orientation was found to be the most frequently used (47.3%), followed by transverse and coronal orientation (3.1% and 2.7%, respectively) (Figure 3B). It should be noted that 46.9% of the reviewed studies (105 of 224; 89 for caudal spine, 14 for lumbar spine, and 2 for cervical spine) did not indicate their specimen orientation in their paper.

The most frequently histological staining being used for the assessment of rat IVDs was hematoxylin and eosin (H&E) staining with a total number of 170, which represented 51.1% of all cases (Figure 3C). The stainings of safranin-O and/or fast-green (SO/FG) and picrosirius-red and/or alcian-blue (PR/AB) were also commonly used, which represented 27.3% and 9.6% of all cases, respectively. Other stains such as Trichomes, Van Gieson, Toluidine Blue and fast-green/alcian-blue/safranin-O/tartrazine (FAST) were also being used, but with a lesser extent (with 3.9%, 3.3%, 2.1%, and 0.3% of all cases, respectively) (Figure 3C).

A total of 135 studies (60.3%), of the 224 reviewed studies, quantitatively evaluated the severity of degeneration in rat IVDs. Among those 135 studies, the grading systems being used were reviewed, and the grading schemes proposed by Han et al[6,41] and Masuda et al[42] were the most popular (26.7% and 24.4%, respectively) (Figure 3D). These grading systems showed high similarities and included degenerative features including NP cellularity and morphology, AF morphology, and NP-AF border (Table 2). Both had a grading range from 1 to 3 for each criterion with 1 indicating normal IVD properties and 3 indicating severe IVD degenerative changes.

TABLE 1 The initial proposed degeneration grading system for rat intervertebral disc

Category	Features	Score	Description	Reference
NP morphology	NP shape	0	Round shape	Han (2008) Mao (2011)
		1	Rounded with mild distortion	
		2	irregular shape	
	NP area	0	NP constitutes more than 50% of disc area	
		1	NP constitutes 50% to 25% of disc area	
		2	NP constitutes less than 25% of disc area	
NP cellularity	Cell number	0	Normal number of nuclear cells	Han (2008) Masuda (2004) Keorochana (2010)
		1	Slight decrease in number of cells (<50)	
		2	Moderate or severe decrease (≥50%) in number of cells	
	Cell clustering and morphology	0	Large vacuolated nuclear cells evenly distributed throughout NP	
		1	Less than one-third of NP cells are clustered and non-vacuolated	
		2	More than one-third of NP cells are clustered and non-vacuolated	
NP-AF border	Border appearance	0	Normal, without any interruption	Han (2008) Masuda (2004)
		1	Minimal interruption, loss of distinction between NP and AF	
		2	No distinction between NP and AF	
AF morphology	Lamellar organization	0	Discrete, well-organized collagen lamellae bulging outward with no infolding	Han (2008) Masuda (2004) Norcross (2003) Mao (2011) Keorochana (2010)
		1	Some (<1/3) distorted or disorganized collagen lamellae with minimal (<1/3) infolding	
		2	Apparent (≥1/3) distorted or disorganized collagen lamellae with moderate to severe (≥1/3) infolding	
	Tears/fissures/disruptions	0	No ruptured or serpentine fibers	
		1	Ruptured or serpentined patterned fibers in less than 1/3 of the anulus	
		2	Ruptured or serpentined patterned fibers in more than 1/3 of the anulus	
AF cellularity	Cell morphology	0	Elliptical cells comprise more than 75% of the cells	Han (2008) Mao (2011)
		1	Mix of elliptical and rounded cells	
		2	Rounded cells comprise more than 75% of the cells	
Endplate	Disruptions/ microfractures & osteophyte/ ossification	0	Continuous endplate with no osteophyte or endplate ossification	Mao (2011) Wang (2004)
		1	Endplate with minimal disruption (<1/3), mild osteophyte or mild endplate ossification (<1/3)	
		2	Endplate with moderate or severe disruption (≥1/3), overgrowth of osteophyte or significant endplate ossification (≥1/3)	
Intradiscal proteoglycan	Proteoglycan intensity	0	Deep proteoglycan stain in peri-NP region; deep and consistent proteoglycan stain between AF lamellae with gradual fading from inner AF towards outer AF	Norcross (2003)
		1	Less prominent proteoglycan stain in peri-NP region; small (<1/3) areas of faded and/or inconsistent proteoglycan stain centrally or in AF	
		2	No prominent proteoglycan stain in peri-NP region; large (≥1/3) areas of faded and/or inconsistent proteoglycan stain centrally or in AF	

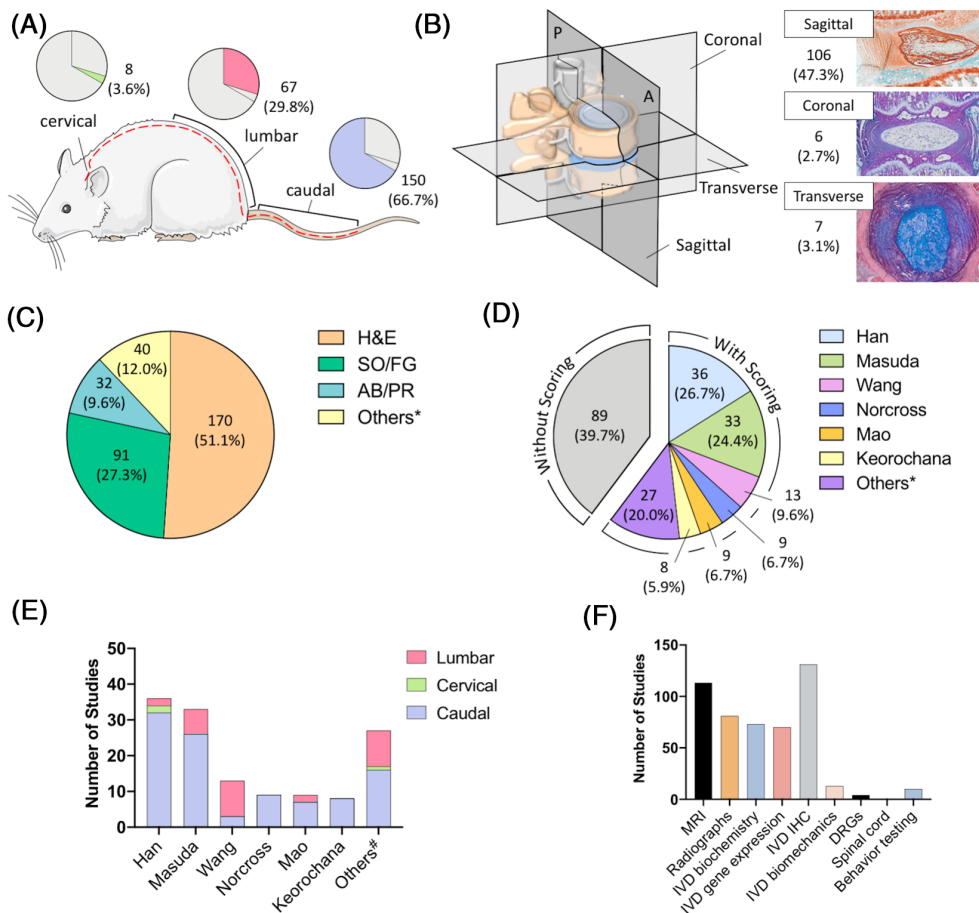Abbreviations: AF, Annulus fibrosus; NP, nucleus pulposus.

FIGURE 3 Literature review about current histological analysis strategies for assessing degeneration of rat IVD specimens. These include spine region, A, specimen orientation, B, types of staining, C, and existing scoring system used for histopathological evaluation, D. Han (2004), Norcross (2003), and Keorochana (2010) scales are more commonly adopted for grading caudal IVDs, while Masuda (2008) and Wang (2004) are more widely used for grading lumbar IVDs, E. Additional outcome measures are commonly performed alongside histological assessment, F. H&E, hematoxylin and eosin; SO/FG, safranin-O/Fast-green; and AB/PR, picrosirius-red/alcian-blue

However, the grading scale by Han et al[41] also included AF cellularity, resulting in a scale range from 5 to 15. Other grading systems being used included schemes by Wang et al[43] (9.6%), Norcross et al[46] (6.7%), Mao et al[6] (6.7%) and Keorochana et al[27] (5.9%), or other scales (20%) (Figure 3D). Some of these grading scales also included criteria assessing the IVD CEP (Mao et al[6]), the appearance of osteophytes (Wang et al[43]), and intradiscal proteoglycan staining intensity (Norcross et al[46]) (Table 2). Among these grading systems, the analysis also showed the schemes by Han et al,[41] Masuda et al,[42] Norcross et al,[46] Mao et al,[6] and Keorochana et al[27] were mainly used to evaluate degeneration in rat caudal IVDs, in which the system by Masuda et al[42] was also used to score rat lumbar IVD. On the other hand, the system by Wang et al[43] was predominately used to grade rat lumbar IVDs (Figure 3E).

In addition to IVD histology, the category (ie, s) of other outcome measures were reviewed. Immunohistochemical analysis was the most common additional measurement for IVD assessment (131 times) (Figure 3F). This analysis could help to identify and localize the specific extracellular matrix, pro-inflammatory cytokines, receptors and signaling pathways in the process of IVD degeneration and/or regeneration. Different studies might use different markers depending on the focus on individual studies. Moreover, MRI (113 times) and radiographs (81 times) were commonly used to visualize the IVD (mainly in vivo, sometimes postmortem), which facilitates a continuous monitoring of IVD changes and a comparison with clinical outcomes. Additionally, IVD biochemistry (73 times), gene expression analysis (70 times) and IVD biomechanics (13 times) were also being used for evaluating different characteristics of the IVD (Figure 3F). In a limited number of cases, pain-associated behaviors and nervous systems in rats were assessed, which facilitates studying the relationship between IVD degeneration and discogenic pain. However, only 10, 4, and 0 studies assessed pain-associated behaviors, the dorsal root ganglion, and the spinal cord respectively, suggesting that this area was insufficiently investigated.

3.2 | Aim 2: Survey study

Information about preferences regarding sample processing and IVD degeneration were assessed from experts in the field. A survey was sent out to the ORS community and >200 corresponding authors from studies included in aim 1 of this work (literature review study). A total of 30 responses were received and evaluated. With 30 respondents, this was considered an informed opinion on those morphological categories and degenerative features to be included in the degeneration grading system.

Different approaches for specimen preparation were compared (Figure 4). Paraffin was most common with 24 out of 30 respondents

TABLE 2 Comparison of different morphological features of intervertebral disc (IVD) degeneration among different existing grading systems

	Han (2004) Grade/Score	Description	Masuda (2008) Grade/Score	Description	Wang (2004) Grade/Score	Description	Norcross (2003) Grade/Score	Description	Mao (2011) Grade/Score	Description	Keorochana (2010) Grade/Score	Description
NP morphology/ matrix	1	Round, comprising at least half of the disc area in midsagittal sections	1	Normal gelatinous appearance	0	Bulging gel with abundant notochordal cells	1	Large, bulging central cavity with abundant NP material; >2/3 IVD height; smooth borders with minimal disruption	1	Round shape and the NP constitutes more than 50% of the disc area	N/A	
					1	Notochordal cells loss; chondrocyte-like cells emergence	2	Slightly reduced central cavity size with some NP material present; >1/3 IVD height and < 2/3 IVD height; minimal border disruption may be present				
	2	Rounded or irregularly shaped, comprising one quarter to half of the disc area in midsagittal sections	2	Slight condensation of the extracellular matrix	2	Focal mucoid degeneration; clefts	3	Markedly reduced and disrupted cavity with minimal NP material and compartmentalization; total cavity >1/3 IVD height and < 2/3 IVD height	2	Intermediate morphology; the NP constitutes 50% to 25% of the disc area		
	3	Irregularly shaped, comprising less than one quarter of the disc area in midsagittal sections	3	Moderate/severe condensation of the extracellular matrix	3	Diffuse mucoid degeneration and clefts throughout nucleus	4	Severe disruption of NP with minimal cavity; total cavity <1/3 IVD height but >O; consists only of a few small pockets lined by NP-like cells	3	Irregular shape and the NP constitutes less than 25% of disc area		
							5	Complete obliteration of cavity with no NP-lined pockets				
NP cellularity	1	Normal cellularity with stellar shaped nuclear cells evenly distributed throughout the nucleus	1	Normal cellularity with large vacuoles in the gelatinous structure of the matrix	N/A		N/A		1	Stellar-shaped cells with a proteoglycan matrix located at the periphery, evenly distributed	0	Normal cellularity with large vacuoles and stellar-shaped nucleus consistently dispersed in the nucleus
	2	Slight decrease in the no. of cells with some clustering	2	Slight decrease in the number of cells and fewer vacuoles					2	Partially stellar and partially round cells, more stellar than round	1	Slight decrease in the number of cells (<50%) with/without cell clustering
	3	Moderate or severe decrease (50%) in the number of cells with all the remaining cells clustered and separated by dense areas of proteoglycans	3	Moderate/severe decrease (50%) in the number of cells and no vacuoles					3	Mostly large, round cells, separated by dense areas of proteoglycan matrix	2	Moderate to severe decrease in the number of cells (>50%) with mostly no vacuolization and occupied by proliferative CNT (<50% of nucleus area)
											3	Severe replacement by proliferative CNT (>50% of nucleus area) with small area of vacuole cells
NP-AF border	1	Normal, without any interruption	1	Normal	N/A		N/A		N/A		N/A	
	2	Minimal interruption	2	Minimally interrupted								
	3	Moderate or severe interruption	3	Moderate/severe interruption								

(Continues)

TABLE 2 (Continued)

	Han (2004)	Masuda (2008)	Wang (2004)	Norcross (2003)	Mao (2011)	Keorochana (2010)
AF morphology	1 — Well-organized collagen lamellae without ruptured or serpentine fibers; 2 — Inward bulging, ruptured or serpentine fibers in less than one third of the annulus; 3 — Inward bulging, ruptured or serpentine fibers in more than one third of the annulus	1; 2; 3 (same criteria as Han)	0 — Normal, pattern of fibrocartilage lamellae without ruptured fibers and without a serpentine appearance anywhere within the anulus; 1 — Ruptured or serpentined patterned fibers in less than 30% of the anulus; 2 — Ruptured or serpentined patterned fibers in more than 30% of the anulus	1 — Compact fibrous lamellas; 2 — Proliferation of fibrocartilaginous tissue and loss of nuclear-annular border; 3 — Fissures in annulus fibrosis; 4 — Severe infolding and distortion of poorly opposed lamellae; severe fragmentation of lamellae; small regions of disorganized fibrous material replacing central lamellae; 5 — Severe infolding, distortion, and fragmentation of lamellae; extensive amount of disorganized fibrous material replacing central lamellae	1 — Discrete, well-opposed lamellae bulging outward with no infolding; minimal preparation defect with "simple radial clefting"; 2 — Discrete lamellae, less well-opposed; minimal infolding may be present; fibers remain well-organized, but with "complex radial clefting"; 3 — Moderate to severe infolding of discrete, relatively well-opposed lamellae; moderate fragmentation of lamellae; AF fibers remain well organized	0 — Well-organized fibrous lamellae without ruptured or serpentine fibers; 1 — Ruptured or serpentine fibers in less than 30% of the annulus; 2 — Ruptured or serpentine fibers in more than 30% of the annulus with reversed contour; 3 — Indistinct and disorganized annulus
AF cellularity	1 — Fibroblasts comprise more than 75% of the cells; 2 — Neither fibroblasts nor chondrocytes comprise more than 75% of the cells; 3 — Chondrocytes comprise more than 75% of the cells	N/A	N/A	N/A	1 — Fibroblasts comprise more than 75% of the cells; 2 — Intermediate; 3 — Chondrocytes comprise more than 75% of the cells	N/A
Proteoglycan staining	N/A	N/A	N/A	1 — Deep blue stain in peri-NP region; deep blue stain between AF lamellae with gradual fading in periphery; 2 — Pattern of stain similar to grade 5, but with less prominent peri-NP stain and more rapid fading of stain between AF lamellae; 3 — Normal pattern no longer present; large areas of faded blue centrally and in AF, but inconsistent and patchy	N/A	N/A

TABLE 2 (Continued)

	Han (2004)	Masuda (2008)	Wang (2004)	Norcross (2003)	Mao (2011)	Keorochana (2010)
				4 — Only 1-3 small patches of faded blue stain either centrally or in AF; 5 — Entire IVD completely washed out with no blue stain	1 Continuous; 2 Disrupted	
Endplate	N/A	N/A	N/A	N/A		N/A
Osteophyte	N/A	N/A	0 Absence; 1 Appearance; 2 Overgrowth	N/A	N/A	N/A
Score range	5-15	4-12	0-7	3-15	5-14	0-3

Abbreviations: AF, Annulus fibrosus; NP, nucleus pulposus.

(80.0%), followed by optimal cutting temperature (OCT) compound (10.0%) and methyl methacrylate (3.3%) (Figure 4A). Two respondents (6.7%) did not have any opinion or did not feel he/she had enough expertise for this question. Consistent with results of the literature review, the most preferable specimen orientation was found to be sagittal with 20 votes (66.7%). Coronal and transverse orientation was chosen by 5 and 4 respondents, respectively (16.7% and 13.3%), whereas one person did not indicate an opinion (3.3%) (Figure 4B). With many different specimen thicknesses proposed, different ranges were defined to bundle multiple answers; 86.7% of all respondents (26 of 30) preferred to use thin sections (<10 μm) for rat IVD specimens. Specifically, 14 of the 26 respondents preferred the sections ranging 3 to 5 μm, while 12 of the 26 respondents preferred the sections ranging 6 to 10 μm (Figure 4C). One respondent indicated a specimen thickness of >10 μm and 3 had no opinion (3.3% and 10.0%, respectively). Similar to the specimen orientation, the histological staining preference was consistent with the results from the literature with the highest number of responses for H&E (25) and SO/FG (27), followed by PR/AB with 12 respondents (Figure 4D).

In order to develop a standardized degeneration grading system for rat IVDs, the survey also included questions about different criteria, their importance, and the general scoring procedure (Figure 5). NP morphology, AF morphology, and NP-AF border appeared to be the most important criteria for scoring IVD degeneration. A total of 26, 24, and 23 (out of 30) respondents, respectively, gave at least 4-point (5-point indicates most important). On the other hand, AF cellularity was given the least importance with 20 respondents given 3-point or less (Figure 5A). The NP cellularity and CEP were ranked intermediate regarding their importance, and 20 respondents gave at least 4-point for both categories. When evaluating severity of IVD degeneration, different degenerative features regarding different IVD regions should be defined and decided whether to be included in the scoring system. For NP morphology, the features of proteoglycan intensity, NP shape, and defects/fissures were shown to have high response rates with 21, 26, and 22 respondents, respectively. Only five respondents had no opinion (Figure 5B). Similar findings were observed for the feature of AF morphology with high response rate for lamellar organization (29 respondents) and tears/fissures/disruptions (25 respondents). Only one participant had no opinion (Figure 5C). With regard to cellularity in NP and AF, the cell clustering was rated as the most important degenerative feature (24 respondents), followed by cell number (22 respondents), cell morphology (20 respondents), and presence/absence of notochordal cells in the NP region (14 respondents). Four respondents had no opinion (Figure 5D). For the CEP, CEP disruptions or microfractures was suggested to be the most important feature with 28 responses, followed by CEP thickness with 22 responses (Figure 5E). Features like CEP cellularity, osteophytes, and bony sclerosis (12, 15, and 16 responses, respectively) were found to be less important based on the responses from the survey. Four participants had no opinion on CEP features.

The survey reflected that there was no clear preference for number of points for each feature (Figure 5F), although an odd number of points for each feature seemed to be favored with 10 responses
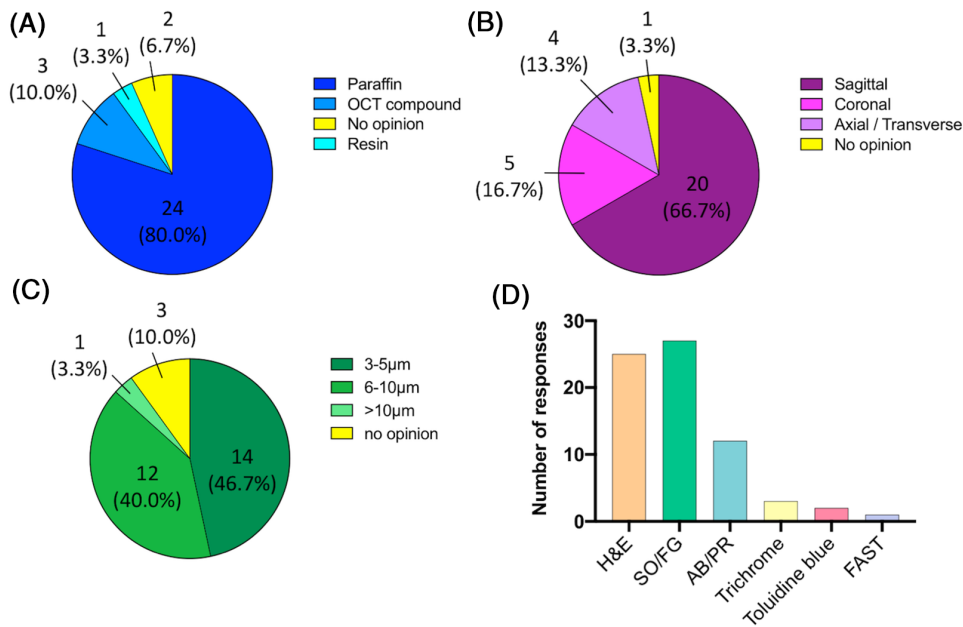
FIGURE 4 Survey study results about different approaches to prepare rat IVD specimens for histopathological analysis. These include embedding media, A, specimen orientation, B, section thickness, C, and types of staining, D. Results are presented as the number of responses (percentage of the whole). OCT compound, optimal cutting temperature compound; H&E, hematoxylin and eosin; SO/FG, safranin-O/Fast-green; AB/PR, picrosirius-red/alcian-blue; and FAST, fast-green/alcian-blue/safranin-O/tartrazine

(33.3%) for a 3-point scale and 11 responses (36.7%) for a 5-point scale. Only six responses were given to a grading scale of 4 points for each feature (20%). Three respondents had no opinion (10%). The number of raters for grading the IVD samples are preferred to be 2 or 3 (both 12 of 30 respondents), whereas 4 or 5 raters was only preferred by 6.7% of the survey participants (2 respondents). Two respondents had no opinion on the number of raters (Figure 5G).

In addition to IVD histology, this survey also gathered information about which outcome measurements should be included in future studies to comprehensively evaluate IVD degenerative changes (Figure 6). Twenty-three respondents suggested including MRI images, which is a gold standard to evaluate IVD degeneration in clinical settings, and also allow to visualize the spine and IVD structures longitudinally at different experimental time points. Other evaluations such as radiographs, microCT, gene expression, and others have a similar response rate between 10 and 15 respondents (Figure 6).

3.3 | Aim 3: Validation study

Combining the literature review and survey results as well as the inputs from the focus group, a grading scheme consisting of seven categories with 10 degenerative features was proposed (Table 1). The proposed degeneration grading system was evaluated using inter- and intra-rater reliability tests, and the results were analyzed separately between experienced and inexperienced graders (Table 3A). For the inter-rater reliability test, the ICCs for the overall degeneration score as well as individual degenerative features were determined. The ICC (1, 3) for the overall score among all raters was 0.79 (95% CI: 0.68-0.88), indicating good agreement between graders. The ICCs for the experienced graders was slightly higher than that of inexperienced graders, 0.81 (95% CI: 0.69-0.90) and 0.76 (95% CI: 0.65-0.87), respectively. The results revealed that the gradings from experienced

graders were more reliable, and the reliability could be improved with experience. Moreover, moderate (0.5 < ICC < 0.75) to good (0.75 < ICC < 1.0) agreement was observed for the degenerative features of NP shape, NP area, NP cell number, NP-AF border, AF lamellar organization and AF tears/fissures/disruptions. However, NP cell clustering and morphology, AF cell morphology, CEP disruptions/microfractures and osteophyte/ossification, and intradiscal proteoglycan intensity showed poor agreement with ICC < 0.5 (Table 3A). For intra-rater reliability testing, the ICCs for the overall scores among the experienced graders ranged from 0.90 (95% CI: 0.79-0.96) to 0.99 (95% CI: 0.99-1.00), which were slightly higher than those among inexperienced graders ranged from 0.80 (95% CI: 0.60-0.91) to 0.98 (95% CI: 0.96-0.99) (Table 3B). The findings indicated good (0.75 < ICC < 1.0) to excellent (ICC > 0.9) agreement between the two scoring sessions for all graders, but also revealed that the scores obtained from experienced graders were relatively more reproducible.

Based on the results of the ICCs, the results from the survey as well as the feedback from graders and the focus group, the degenerative features of AF cell morphology and intradiscal proteoglycan intensity were considered to be excluded from the grading system. Interestingly, the ICCs among all graders and experienced graders were slightly improved when these two features were removed, with 0.80 (95% CI: 0.70-0.89) and 0.84 (95% CI: 0.75-0.92), respectively (Table 3A). Besides, the language of the grading system and the example images were refined to further clarify the features to be scored in the categories with poor ICC. The final scoring system is summarized in Table 4, and example images for individual category and feature are provided in Figure 7.

4 | DISCUSSION

This study established a standardized, reliable histological grading system for quantifying IVD degeneration in different rat models. With

FIGURE 5 Survey study results about the degeneration grading system for rat IVDs. These include the importance, A, morphological features, B-E, and number of points, F, of different categories in the grading system, as well as the number of grader(s) should be involved, G. For the importance of different categories, A, 5 indicates the most important; while 1 indicates the least important. The results suggest nucleus pulposus (NP) morphology, NP cellularity, annulus fibrosus (AF) morphology, NP-AF border, and endplate (EP) should be prioritized to be included in the grading system. B-E, shows features for NP morphology, AF morphology, NP or AF cellularity, and endplate, respectively. PG, proteoglycan
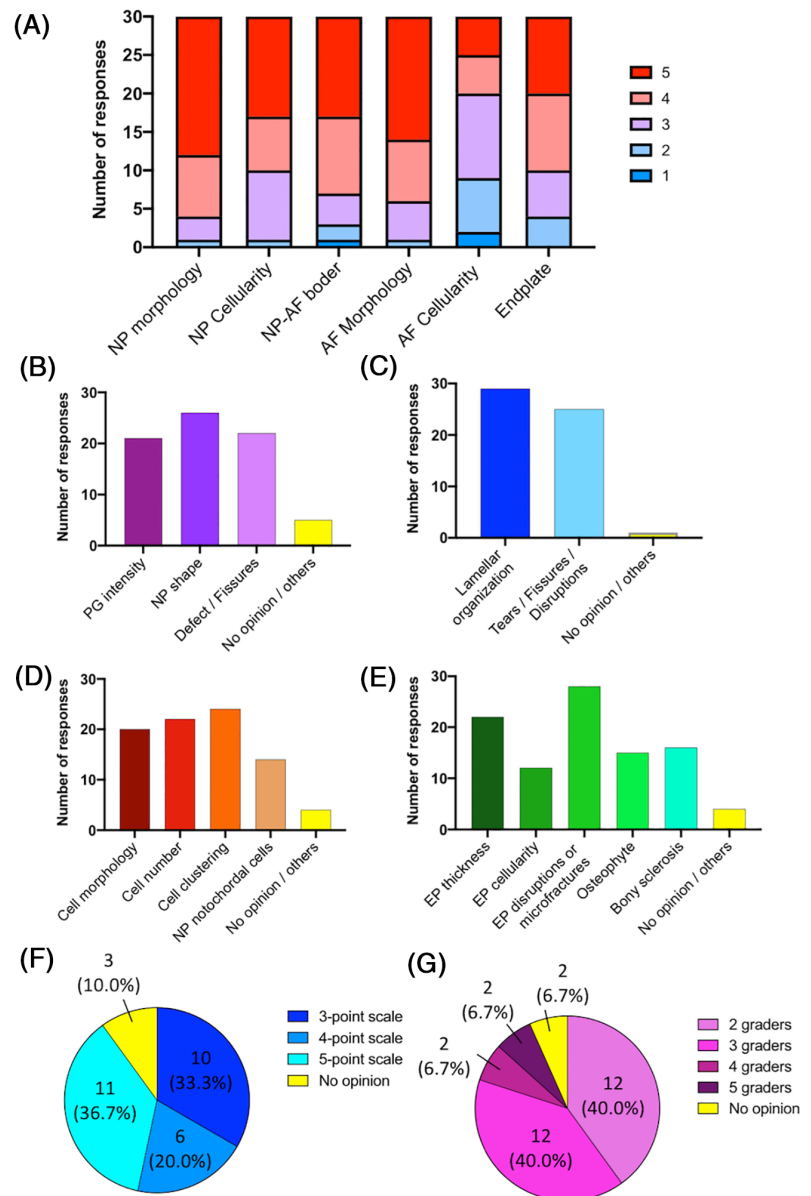
efforts initiated by the ORS spine section, broad outreach in the survey, discussions with the focus group, and international participation in the grading validation, it is hoped that this grading system will be widely-accepted in order to enable more objective comparison between experimental groups within a single study and across different studies and laboratories. The literature review (Aim 1) and the survey (Aim 2) were used to identify 7 categories and 10 degenerative features important for quantifying different severities of degeneration in rat IVDs. The inter- and intra-rater reliability results (Aim 3) showed good to excellent agreement and high reproducibility (both ICC > 0.75), revealing the initial proposed grading system (Table 1) was generally easy to be adopted for both experienced and inexperienced graders. In this validation test, we used histological slides of lumbar and coccygeal IVD samples with different degeneration models (including annular injury, nucleotomy, or mechanical compression) collected from eight different research groups of different

institutions. The high agreement therefore suggests this grading system can be applied for a variety of rat IVD samples and degeneration models. However, the proposed grading system will need future studies to validate for different rat strains, age and sex, and to adjust for evaluating regenerative changes. Moreover, it should be noted that the ICCs for experienced graders were slightly higher than those for inexperienced graders, suggesting the history of experience working with rat IVD histology improved the reliability of grading. Training sessions and practice are therefore highly recommended for inexperienced researchers prior to IVD degeneration scoring.

Based on the results of the ICCs, the results from survey as well as the feedback from graders and focus group, the grading system was refined by excluding some degenerative features with poor agreement (ICC < 0.5) in the inter-rater reliability test and revising the descriptions and the example images of the grading system. A final consensus degeneration grading system with five categories and eight
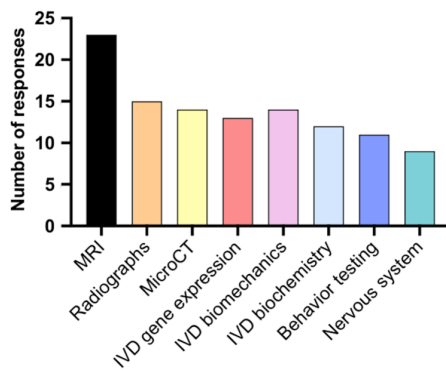
FIGURE 6 Survey study results about additional outcome measures should be included for assessing different properties of rat IVDs. IVD, intervertebral disc; MRI, magnetic resonance imaging; and CT, computed tomography

degenerative features (with 3-point scale, that is, score 0-2, for each feature, and the overall score between 0 and 16) was proposed (Table 4). This grading system was integrated and modified from existing grading systems by Han et al,[41] Masuda et al,[42] Mao et al,[6] Keorochana et al,[27] Norcross et al,[46] and Wang et al[43] (Table 2). Each morphological category was equally weighted in the existing grading systems; while the proposed system weighs certain categories more by including more than one degenerative features in contributing to the overall degeneration score. Specifically, NP and AF morphology each include two degenerative features since they were ranked to be highly important in the survey (Figure 5A). Alterations in notochordal cell morphology is an important and easily identifiable feature in degenerative rat IVDs, so the NP cellularity category is also weighted twice with two features. The proposed grading system consists of a more comprehensive list of morphological categories and features that builds off prior systems and is expected to better identify a wider scope of degenerative changes and to facilitate the evaluation of different severities of IVD degeneration. The ICCs of the reliability tests identified in this study are generally comparable with those reported from the Osteoarthritis Research Society International (OARSI) scoring system developed for grading osteoarthritis in rats (ICCs ranging from 0.44 to 0.99 depending on category and experience level of grader) and rabbits (ICCs ranging from 0.82 to 0.99 depending on category and experience level of grader).[47,48] Moreover, a 3-point scale was used for each category in the grading system to balance resolution of the grading system with easy adoption by users. Objectivity can be improved by increasing the numbers of graders, and the survey indicated that 2 or 3 graders was widely accepted for grading IVD degeneration using the semi-quantitative grading systems to eliminate preference and potential bias of individual graders. Scores obtained from individual graders are recommended to be averaged for statistical analysis.

It should be noted that the overall score of the revised grading system (Table 4) could help to differentiate non-degenerated and degenerated IVDs. The averaged overall score for non-degenerated healthy IVDs (ie, from naive or sham surgery groups) was 2.8 (±2.2),

while the average score for degenerated IVDs was 9.0 (±2.9). Besides, when further subdividing the IVDs with degenerative phenotypes into different severities of degeneration, that is, mild, moderate and severe, according to the histology, their averaged scores were 6.0 (±1.5), 8.7 (±1.0), and 12.1 (±1.7), respectively, revealing that this grading system can be used to identify different severity of IVD degeneration. Together, it is suggested that the scores between 0 and 3, 4 and 7, 8 and 11, and 12 and 16 are identified as non-degenerated, mild, moderate, and severe degenerated IVDs, respectively. Moreover, the overall scores between experienced and inexperienced graders were also compared. For the experienced graders, the average score for non-degenerated and degenerated IVDs were 3.0 (±2.4) and 9.1 (±2.9), respectively; while for inexperienced graders, the average score were 2.7 (±2.1) and 8.9 (±2.9) for non-degenerated and degenerated IVDs, respectively. This finding revealed that there was no obvious difference in overall score between experienced and inexperienced graders, although the scores obtained from the experienced graders were slightly more reproducible than those from inexperienced graders.

This study reviewed sample preparation methods to minimize histological variations that might affect the results of degeneration grading. For specimen orientation, both literature review and survey study showed that the sagittally oriented specimens were mostly preferred for IVD histology analysis (Figure 3B and 4B). The structures of NP, AF, and CEP of IVD as well as the adjacent vertebrae can be clearly visualized in the sagittal-oriented IVD specimens, which helps to identify degenerative changes in different IVD regions. These features remain hidden when the specimens are oriented transversely. However, transverse-oriented specimens have the benefit of faster processing as decalcification is not required and easier sectioning. Sagittal-orientation is considered preferable to coronally-oriented specimens because degenerative changes in anterior vs posterior regions, and sagittal curvature can be discerned. After tissue fixation, the oriented samples are embedded in one of the three most common embedding media for sectioning: paraffin, OCT compound or methyl methacrylate (resin), with paraffin being the most preferred for rat IVD (Figure 4A). Paraffin-embedded samples are relatively easier to section compared with resin-embedded samples, and the morphological structure shows fewer histology artifacts than the samples embedded in the OCT compound. However, decalcification can be avoided for sectioning the resin-embedded specimens, which makes it a better alternative to assess CEP calcification. There was no absolute agreement for the sectioning thickness among the survey responders. However, more than 85% respondents reported to use thin section (less than 10 μm), and only one respondent reported to use thick section (20 μm) for cryosectioning of OCT-embedded specimens, indicating that a section thickness < 10 μm is widely accepted. Taken together, we suggest embedding the samples in sagittal orientation using paraffin, and sectioning for thin specimens (< 10 μm) to improve comparability between different research groups.

H&E and SO/FG stains were identified as a clear preference to visualize the microanatomy of rat IVDs from the literature review and survey study. For H&E, the hematoxylin stains cell nuclei blue, which

TABLE 3 Intraclass correlation coefficients (ICCs) for inter- (A) and intra-rater (B) reliability test

(A)

	Category	Experienced raters (n = 5)	Inexperienced raters (n = 10)	All raters (n = 15)
ICCs for individual morphological feature	NP shape	0.828 (0.723-0.909)	0.63 (0.488-0.776)	0.676 (0.549-0.806)
	NP area	0.749 (0.612-0.862)	0.606 (0.462-0.758)	0.759 (0.528-0.794)
	NP cell number	0.576 (0.401-0.747)	0.508 (0.361-0.682)	0.537 (0.398-0.7)
	NP cell clustering & morphology	0.381 (0.203-0.592)	0.483 (0.336-0.661)	0.465 (0.329-0.639)
	NP-AF border	0.632 (0.465-0.786)	0.665 (0.529-0.801)	0.655 (0.525-0.792)
	AF lamellar organization	0.71 (0.561-0.838)	0.623 (0.481-0.771)	0.647 (0.515-0.786)
	AF tears/fissures/disruptions	0.471 (0.29-0.668)	0.58 (0.435-0.739)	0.562 (0.424-0.721)
	AF cell morphology	0.242 (0.083-0.461)	0.473 (0.326-0.652)	0.411 (0.279-0.589)
	Endplate disruptions/osteophyte	0.538 (0.36-0.719)	0.381 (0.242-0.568)	0.435 (0.301-0.611)
	Intradiscal PG Intensity	0.28 (0.114-0.499)	0.289 (0.164-0.474)	0.319 (0.201-0.496)
ICC for overall score		0.806 (0.691-0.896)	0.763 (0.649-0.866)	0.785 (0.682-0.879)
ICC for overall score (exclude AF cell morphology & intradiscal PG intensity)		0.843 (0.745-0.917)	0.762 (0.647-0.865)	0.795 (0.695-0.885)

(B)

Graders	ICC for overall score				
Experienced	0.955 (0.90-0.98)	0.994 (0.99-1.00)	0.903 (0.79–0.96)	0.983 (0.96-0.99)	0.984 (0.96-0.99)
Inexperienced	0.958 (0.91-0.98)	0.937 (0.86-0.97)	0.884 (0.76-0.96)	0.979 (0.95-0.99)	0.98 (0.96-0.99)
	0.976 (0.95-0.99)	0.799 (0.60-0.91)	0.987 (0.97-0.99)	0.931 (0.85-0.97)	0.922 (0.83-0.97)

Abbreviations: AF, annulus fibrosus; PG, proteoglycan; NP, nucleus pulposus.

helps identifying IVD cells, particularly the NP cells, for grading the category of NP cellularity in the degeneration grading system. Eosin stains extracellular matrix and cytoplasm, including proteoglycans and collagens in pink with a good contrast to the hematoxylin for sufficient separation from the nuclei. On the other hand, the safranin-O stains proteoglycans, chondrocytes and type II collagen red, while the fast-green counterstains the non-collagen components and provides a clear contrast to the safranin-O staining. The two stainings can be performed on separate sections, or for simplicity, hematoxylin can be combined sequentially with SO/FG staining in single section (ie, safranin-O/fast-green/hematoxylin).[5,7,13]

Broader characterization of degenerative changes can include additional modalities and non-histological outcome measurements. MRI is widely used in human clinical practice and research to assess IVD degeneration and spine pathological changes, and is commonly used to evaluate rat IVDs in the pre-clinical setting (Figures 3F and 6). MRI is a non-invasive measurement that is also capable of documenting IVD changes at different stages during an experiment to identify important time point(s) for IVD degeneration progression and effects of therapeutic interventions. MRI methods are continuously improving and have sufficient resolution to visualize the gross IVD structures and to assess water, collagen, and proteoglycan

TABLE 4 The modified and final consensus degeneration grading system for rat intervertebral discs (IVDs)

Category	Features	Score	Description	Reference
NP morphology	NP shape	0	Round/oval shape	Han (2008) Mao (2011)
		1	Round/oval with mild distortion	
		2	Irregular shape	
	NP area	0	NP constitutes more than 40% of disc area	
		1	NP constitutes 40% to 20% of disc area	
		2	NP constitutes less than 20% of disc area	
NP cellularity	Cell number	0	Normal number of nuclear cells (NP cells comprise more than 2/3 of NP space)	Han (2008) Masuda (2004) Keorochana (2010)
		1	Slight decrease in number of cells (NP cells comprise 2/3 to 1/3 of NP space)	
		2	Moderate or severe decrease in number of cells (NP cells comprise less than 1/3 of NP space)	
	Cell morphology	0	More than 80% of nuclear cells are large and vacuolated	
		1	80% to 30% of nuclear cells are large and vacuolated	
		2	Less than 30% of nuclear cells are large and vacuolated	
NP-AF border	Border appearance	0	Normal, clear distinction between NP and AF	Han (2008) Masuda (2004)
		1	Minimal interruption, loss of distinction between NP and AF	
		2	No distinction between NP and AF	
AF morphology	Lamellar organization	0	Discrete, well-organized collagen lamellae bulging outward (less than 20% of annular lamellae are infolding, distorted, disorganized or serpentined)	Han (2008) Masuda (2004) Norcross (2003) Mao (2011) Keorochana (2010)
		1	20% to 60% of annular lamellae are infolding, distorted, disorganized or serpentined	
		2	More than 60% of annular lamellae are infolding, distorted, disorganized or serpentined	
	Tears/fissures/ disruptions	0	No ruptured fibers	
		1	Ruptured fibers in less than 1/3 of the anulus	
		2	Ruptured fibers in more than 1/3 of the anulus	
Endplate	Disruptions/ microfractures and osteophyte/ ossification	0	Continuous endplate with no osteophyte or endplate ossification	Mao (2011) Wang (2004)
		1	Endplate with minimal disruption (<1/3), mild osteophyte or mild endplate ossification (<1/3)	
		2	Endplate with moderate or severe disruption (≥1/3), overgrowth of osteophyte or significant endplate ossification (≥1/3)	

Abbreviations: AF, annulus fibrosus; NP, nucleus pulposus.

contents.[49,50] Radiography, immunohistochemistry, biochemistry, gene expression and biomechanics are also commonly used for assessing different characteristics of the IVD (Figure 3F), however, <50% of survey respondents recommend their use to quantify IVD degeneration (Figure 6). These additional measurements complement histological findings in testing hypotheses on pathophysiology and identifying mechanisms of effects, yet do not directly reflect IVD degeneration severity. A strength of the rat model is the use of measurements to assess pain-related behaviors. Approximately one-third of survey respondents indicated pain-associated behaviors and nervous systems should be included in an in vivo rat model study, yet less than 1% of the reviewed studies investigated the changes of these two measurements in their studies (Aim 1, Figure 3F). Research on the relationship between IVD degeneration and pain-related behaviors remains underrepresented in rat models, and this important research area remains an pivotal aspect for future investigations.

It is also important to emphasize that the grading system has not been validated for IVD regeneration, which some regenerative
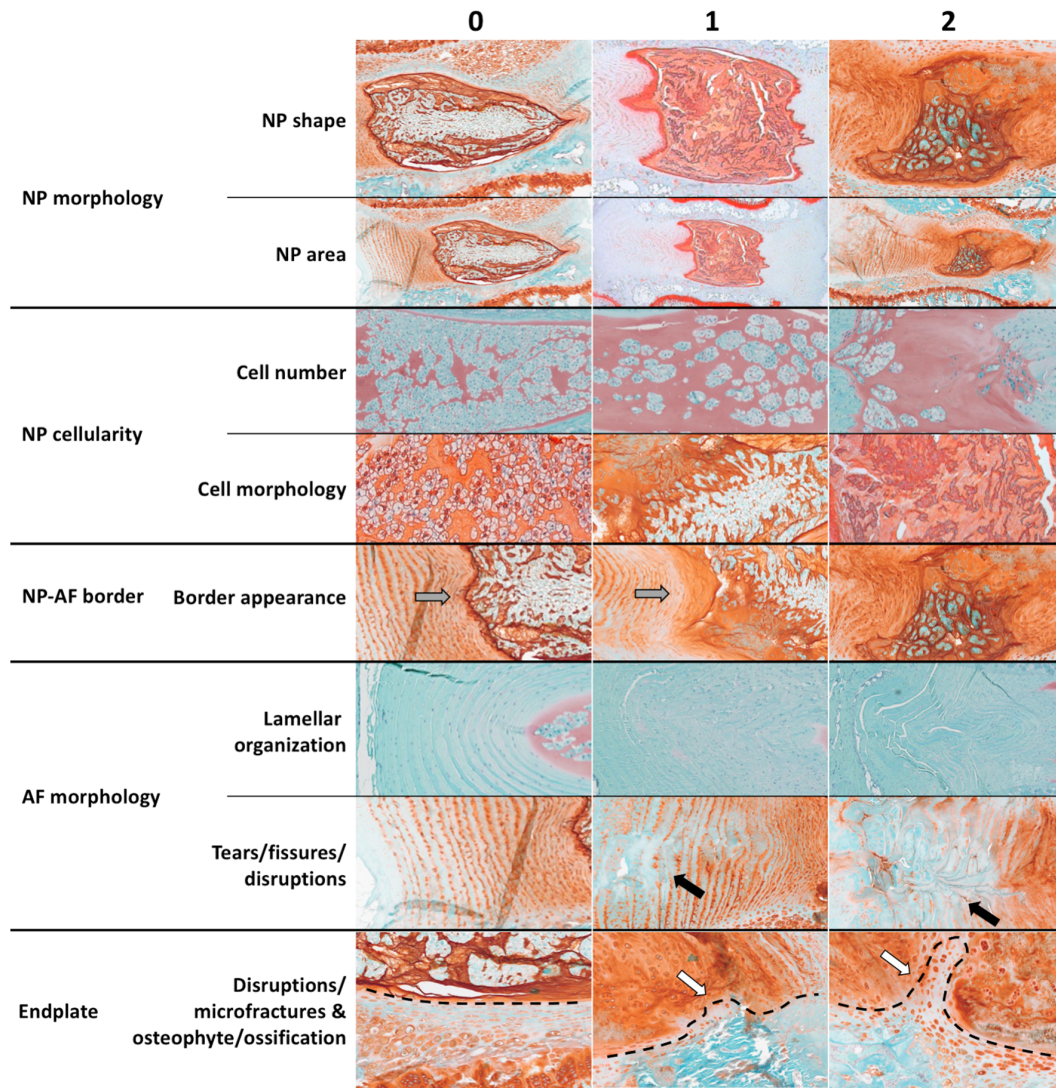
FIGURE 7   Representative images for different categories and features of the modified IVD degeneration grading system. The NP-AF border is the boundary between NP and AF, which is indicated using gray arrows. The AF fissure is a deficiency of one or more layers of the AF, which is highlighted using black arrow. The contour of the endplate is illustrated using black dotted line, and the endplate disruptions are indicated using white arrows. NP, nucleus pulposus; and AF, annulus fibrosus

changes are likely to need adjustments in grading categories. For example, if an IVD degeneration rat model is adopted to determine the efficacy of cell transplantation product or strategy, the transplanted cells will modify cell number and cell morphology in ways that are distinct from the native IVD cells. Similarly, hydrogels or other biomaterial that are intradiscally applied will modify the IVD morphology and hydration, and are not accounted for in current grading categories. Therefore, future refinements of this grading scheme will need to confirm its feasibility to detect regenerative changes and make potential modifications for regenerative changes, as well as cell and biomaterial implantation. Both rat lumbar and coccygeal IVDs are structurally, morphologically and biochemically comparable with human IVDs, and are commonly used for studying IVD degeneration.[2-5] Similar to human IVDs, the rat degenerated IVDs exhibited decreased NP volume, reduced NP cellularity, ruptured and disorganized AF, and a shift towards catabolism with reduced extracellular

matrix production and increased matrix degrading enzymes and pro-inflammatory cytokines.[5,7,12-23] However, it should be noted that large vacuolated notochordal cells occupy the NP of skeletally mature rat IVDs,[37] while this phenotypic differentiation in humans occurs before skeletal maturity in human IVDs. The notochordal cell phenotype is known to enhance proteoglycan synthesis,[51-55] and the presence of notochordal cells in rat IVDs therefore may result in different biochemical and histological changes when compared with human IVDs. The anatomical structures and musculatures of rat spine are similar to human spine, and while rats are quadrupedal, it is known that musculature provides the dominant source for axial compressive loading just like in human spines.[56]

In conclusion, a new grading system for scoring IVD degeneration in rat models (0-16 points) was developed that incorporated categories and degenerative features systematically identified using a literature review, a survey for collecting opinion from experts in the field,

and a validation study using experts and inexperienced graders. The validation study demonstrated that this grading system was generally straightforward and adequately adopted by both experienced and inexperienced graders in a variety of samples (lumbar and coccygeal IVD samples across different degeneration models). A more standardized protocol for the preparation of rat IVD specimens for histological assessment is also recommended which involves embedding IVD samples in paraffin at sagittal orientation, cutting thin sections (<10 μm), and staining with H&E and/or SO/FG. Together, the proposed preparation protocol and grading system are hoped to provide more objective comparisons of histological analyses that facilitate improved comparisons between laboratories and IVD degeneration models.

ACKNOWLEDGMENTS

CONFLICT OF INTEREST

The authors declare no conflicts of interest.

AUTHOR CONTRIBUTIONS

Conception and design of the study: Alon Lai, Jennifer Gansau, Sarah E. Gullbrand, James C. Iatridis. Literature review and analysis: Alon Lai, Jennifer Gansau, Jeffrey Okewunmi. Survey drafting and analysis: Alon Lai, Jennifer Gansau, Sarah E. Gullbrand, James C. Iatridis. Scoring of images for validation and ICC analysis: Alon Lai, Jennifer Gansau, Sarah E. Gullbrand, James Crowley, Carla Cunha, Stefan Dudli, Julie B. Engiles, Marion Fusellier, Raquel M. Goncalves, Daisuke Nakashima, Matthew Pelletier, Steven M. Presciutti, Jordy Schol, Yoshiki Takeoka, Takashi Yurube, Yejia Zhang, James C. Iatridis. Provided histology images and input on scoring system: Alon Lai, Jennifer Gansau, Carla Cunha, Yoshiki Takeoka, Jordy Schol, Sidong Yang, Takashi Yurube, Daisuke Nakashima, James C. Iatridis. Critical review of scoring system: All Authors. Original manuscript draft: Alon Lai, Jennifer Gansau. Critical revisions of manuscript and final approval of the current manuscript: All Authors. Authors performing scoring for validation or who provided images for validations studies are listed alphabetically.

[Correction added 18 June 2021, after first online publication: The fifth author's name, Carla Cunha, has been added as one of contributors to the Provided histology images and input on scoring system under the Author Contributions section.]

DATA AVAILABILITY STATEMENT

The data that support the findings of this study are available from the first author and corresponding author (A. L. and J. C. I., respectively) upon reasonable request.

ORCID

Alon Lai https://orcid.org/0000-0002-0163-4588
Sarah E. Gullbrand https://orcid.org/0000-0001-7806-6606
Daisuke Nakashima https://orcid.org/0000-0003-1105-2669
Matthew Pelletier https://orcid.org/0000-0003-1643-6696
Steven M. Presciutti https://orcid.org/0000-0001-6547-9495
Sidong Yang https://orcid.org/0000-0003-2342-4714
Takashi Yurube https://orcid.org/0000-0002-3007-361X
Yejia Zhang https://orcid.org/0000-0002-7484-8800
James C. Iatridis https://orcid.org/0000-0002-2186-0590

REFERENCES

1. Oichi T, Taniguchi Y, Oshima Y, et al. Pathomechanism of intervertebral disc degeneration. *JOR Spine*. 2020;3(1):e1076.
2. Cunha C, Lamas S, Gonçalves RM, Barbosa MA. Joint analysis of IVD herniation and degeneration by rat caudal needle puncture model. *J Orthop Res*. 2017;35(2):258-268.
3. Cheng X, Zhang G, Zhang L, et al. Mesenchymal stem cells deliver exogenous miR-21 via exosomes to inhibit nucleus pulposus cell apoptosis and reduce intervertebral disc degeneration. *J Cell Mol Med*. 2018;22(1):261-276.
4. Matta A, Karim MZ, Isenman DE, Erwin WM. Molecular therapy for degenerative disc disease: clues from Secretome analysis of the Notochordal cell-rich nucleus pulposus. *Sci Rep*. 2017;7:45623.
5. Evashwick-Rogler TW, Lai A, Watanabe H, et al. Isnhibiting tumor necrosis factor-alpha at time of induced intervertebral disc injury limits long-term pain and degeneration in a rat model. *JOR Spine*. 2018;1(2):e1014. https://doi.org/10.1002/jsp2.1014.
6. Mao H, Chen Q, Han B, et al. Tssshe effect of injection volume on disc degeneration in a rat tail model. *Spine*. 2011;36(16):E1062-E1069.
7. Lai A, Moon A, Purmessur D, et al. Annular puncture with tumor necrosis factor-alpha injection enhances painful behavior with disc degeneration in vivo. *Spine J*. 2016;16(3):420-431.
8. Wu X, Liu Y, Guo X, et al. Prolactin inhibits the progression of intervertebral disc degeneration through inactivation of the NF-κB pathway in rats. *Cell Death Dis*. 2018;9(2):98.
9. Pan Z, Sun H, Xie B, et al. Therapeutic effects of gefitinib-encapsulated thermosensitive injectable hydrogel in intervertebral disc degeneration. *Biomaterials*. 2018;160:56-68.
10. Zhou X, Wang J, Fang W, et al. Genipin cross-linked type II collagen/chondroitin sulfate composite hydrogel-like cell delivery system induces differentiation of adipose-derived stem cells and regenerates degenerated nucleus pulposus. *Acta Biomater*. 2018;71:496-509.
11. Li K, Lv C. Intradiscal injection of sesamin protects from lesion-induced degeneration. *Connect Tissue Res*. 2020;61(6):594-603. https://doi.org/10.1080/03008207.2019.1651847.
12. Mosley GE, Hoy RC, Nasser P, et al. Sex differences in rat intervertebral disc structure and function following annular puncture injury. *Spine*. 2019;44(18):1257-1269.
13. Lai A, Ho L, Evashwick-Rogler TW, et al. Dietary polyphenols as a safe and novel intervention for modulating pain associated with intervertebral disc degeneration in an in-vivo rat model. *PLoS One*. 2019;14(10):e0223435.
14. Zhang J, Li Z, Chen F, et al. TGF-β1 suppresses CCL3/4 expression through the ERK signaling pathway and inhibits intervertebral disc degeneration and inflammation-related pain in a rat model. *Exp Mol Med*. 2017;49(9):e379.
15. Kim J-S, Kroin JS, Li X, et al. The rat intervertebral disk degeneration pain model: relationships between biological and structural alterations and pain. *Arthritis Res Ther*. 2011;13(5):R165.

16. Luo Y, Zhang L, Wang W-Y, Hu QF, Song HP, Zhang YZ. The inhibitory effect of salmon calcitonin on intervertebral disc degeneration in an ovariectomized rat model. *Eur Spine J*. 2015;*24*(8):1691-1701.

17. Makino H, Seki S, Yahara Y, et al. A selective inhibition of c-Fos/-activator protein-1 as a potential therapeutic target for intervertebral disc degeneration and associated pain. *Sci Rep*. 2017;*7*(1):16983.

18. Gruber HE, Hanley EN. Morphologic features of spontaneous annular tears and disc degeneration in the aging sand rat (Psammomysobesusobesus). *Biotech Histochem*. 2017;*92*(6):402-410.

19. Taş U, Caylı S, Inanır A, et al. Aquaporin-1 and aquaporin-3 expressions in the intervertebral disc of rats with aging. *Balkan Med J*. 2012; *29*(4):349-353.

20. Zhang Y, Xia J, Qiu Y, Bai Y. Correlation between osteoporosis and degeneration of intervertebral discs in aging rats. *J Huazhong Univ Sci Technolog Med Sci*. 2012;*32*(2):210-215.

21. Hou G, Lu H, Chen M, Yao H, Zhao H. Oxidative stress participates in age-related changes in rat lumbar intervertebral discs. *Arch Gerontol Geriatr*. 2014;*59*(3):665-669.

22. Chan AK, Tang X, Mummaneni NV, et al. Pulsed electromagnetic fields reduce acute inflammation in the injured rat-tail intervertebral disc. *JOR Spine*. 2019;*2*(4):e 1069.

23. Maerz T, Newton M, Marek AA, Planalp M, Baker K. Dynamic adaptation of vertebral endplate and trabecular bone following annular injury in a rat model of degenerative disc disease. *Spine J*. 2018;*18* (11):2091-2101.

24. Fujii T, Fujita N, Suzuki S, et al. The unfolded protein response mediated by PERK is casually related to the pathogenesis of intervertebral disc degeneration. *J Orthop Res*. 2018;*36*(5):1334-1345.

25. Maidhof R, Rafiuddin A, Chowdhury F, Jacobsen T, Chahine NO. Timing of mesenchymal stem cell delivery impacts the fate and therapeutic potential in intervertebral disc repair. *J Orthop Res*. 2017;*35*(1):32-40.

26. Nakayama E, Matsumoto T, Kazama T, Kano K, Tokuhashi Y. Transplantation of dedifferentiation fat cells promotes intervertebral disc regeneration in a rat intervertebral disc degeneration model. *Biochem Biophys Res Commun*. 2017;*493*(2):1004-1009.

27. Keorochana G, Johnson JS, Taghavi CE, et al. The effect of needle size inducing degeneration in the rat caudal disc: evaluation using radiograph, magnetic resonance imaging, histology, and immunohistochemistry. *Spine J*. 2010;*10*(11):1014-1023.

28. Gruber HE, Johnson T, Norton HJ, Hanley EN. The sand rat model for disc degeneration: radiologic characterization of age-related changes: cross-sectional and prospective analyses. *Spine*. 2002;*27*(3):230-234.

29. Moskowitz RW, Ziv I, Denko CW, Boja B, Jones PK, Adler JH. Spondylosis in sand rats: a model of intervertebral disc degeneration and hyperostosis. *J Orthop Res*. 1990;*8*(3):401-411.

30. Silberberg R, Aufdermaur M, Adler JH. Degeneration of the intervertebral disks and spondylosis in aging sand rats. *Arch Pathol Lab Med*. 1979;*103*(5):231-235.

31. Hirata H, Yurube T, Kakutani K, et al. A rat tail temporary static compression model reproduces different stages of intervertebral disc degeneration with decreased notochordal cell phenotype. *J Orthop Res*. 2014;*32*(3):455-463.

32. Yurube T, Hirata H, Kakutani K, et al. Notochordal cell disappearance and modes of apoptotic cell death in a rat tail static compression-induced disc degeneration model. *Arthritis Res Ther*. 2014;*16*(1):R31.

33. Lai A, Chow DHK. Effects of traction on structural properties of degenerated disc using an in vivo rat-tail model. *Spine*. 2010;*35*(14):1339-1345.

34. Liang T, Zhang L-L, Xia W, et al. Individual collagen fibril thickening and stiffening of annulus fibrosus in degenerative intervertebral disc. *Spine*. 2017;*42*(19):E1104-E 1111.

35. Li Z, Shao Z, Chen S, et al. TIGAR impedes compression-induced intervertebral disc degeneration by suppressing nucleus pulposus cell apoptosis and autophagy. *J Cell Physiol*. 2020;*235*(2):1780-1794.

36. Che Y-J, Guo J-B, Liang T, et al. Controlled immobilization-traction based on intervertebral stability is conducive to the regeneration or

37. repair of the degenerative disc: an in vivo study on the rat coccygeal model. *Spine J*. 2019;*19*(5):920-930.

37. Iatridis JC, Mente PL, Stokes IA, et al. Compression-induced changes in intervertebral disc properties in a rat tail model. *Spine*. 1999;*24*(10): 996-1002.

38. Mac Lean JJ, Lee CR, Grad S, et al. Effects of immobilization and dynamic compression on intervertebral disc cell gene expression in vivo. *Spine*. 2003;*28*(10):973-981.

39. Yurube T, Nishida K, Suzuki T, et al. Matrix metalloproteinase (MMP)-3 gene up-regulation in a rat tail compression loading-induced disc degeneration model. *J Orthop Res*. 2010;*28*(8):1026-1032.

40. Yurube T, Takada T, Suzuki T, et al. Rat tail static compression model mimics extracellular matrix metabolic imbalances of matrix metalloproteinases, aggrecanases, and tissue inhibitors of metalloproteinases in intervertebral disc degeneration. *Arthritis Res Ther*. 2012;*14*(2):R51.

41. Han B, Zhu K, Li F-C, et al. A simple disc degeneration model induced by percutaneous needle puncture in the rat tail. *Spine*. 2008;*33*(18): 1925-1934.

42. Masuda K, Aota Y, Muehleman C, et al. A novel rabbit model of mild, reproducible disc degeneration by an anulus needle puncture: correlation between the degree of disc injury and radiological and histological appearances of disc degeneration. *Spine*. 2005;*30*(1):5-14.

43. Wang T, Zhang L, Huang C, Cheng AG, Dang GT. Relationship between osteopenia and lumbar intervertebral disc degeneration in ovariectomized rats. *Calcif Tissue Int*. 2004;*75*(3):205-213.

44. Rutges JPHJ, Duit RA, Kummer JA, et al. A validated new histological classification for intervertebral disc degeneration. *Osteoarthr Cartil*. 2013;*21*(12):2039-2047.

45. Nishimura K, Mochida J. Percutaneous reinsertion of the nucleus pulposus. An experimental study. *Spine*. 1998;*23*(14):1531-1538.discussion 1539.

46. Norcross JP, Lester GE, Weinhold P, Dahners LE. An in vivo model of degenerative disc disease. *J Orthop Res*. 2003;*21*(1):183-188.

47. Gerwin N, Bendele AM, Glasson S, Carlson CS. The OARSI histopathology initiative - recommendations for histological assessments of osteoarthritis in the rat. *Osteoarthr Cartil*. 2010;*18*(Suppl 3): S24-S34.

48. Laverty S, Girard CA, Williams JM, Hunziker EB, Pritzker KPH. The OARSI histopathology initiative - recommendations for histological assessments of osteoarthritis in the rabbit. *Osteoarthr Cartil*. 2010;*18* (Suppl 3):S53-S65.

49. Bashir A, Gray ML, Hartke J, Burstein D. Nondestructive imaging of human cartilage glycosaminoglycan concentration by MRI. *Magn Reson Med*. 1999;*41*(5):857-865.

50. Nieminen MT, Rieppo J, Töyräs J, et al. T2 relaxation reveals spatial collagen architecture in articular cartilage: a comparative quantitative MRI and polarized light microscopic study. *Magn Reson Med*. 2001;*46* (3):487-493.

51. Aguiar DJ, Johnson SL, Oegema TR. Notochordal cells interact with nucleus pulposus cells: regulation of proteoglycan synthesis. *Exp Cell Res*. 1999;*246*(1):129-137.

52. Hunter CJ, Matyas JR, Duncan NA. Cytomorphology of notochordal and chondrocytic cells from the nucleus pulposus: a species comparison. *J Anat*. 2004;*205*(5):357-362.

53. Purmessur D, Guterl CC, Cho SK, et al. Dynamic pressurization induces transition of notochordal cells to a mature phenotype while retaining production of important patterning ligands from development. *Arthritis Res Ther*. 2013;*15*(5):R122.

54. Risbud MV, Shapiro IM. Notochordal cells in the adult intervertebral disc: new perspective on an old question. *Crit Rev Eukaryot Gene Expr*. 2011;*21*(1):29-41.

55. Bach FC, Tellegen AR, Beukers M, et al. Biologic canine and human intervertebral disc repair by notochordal cell-derived matrix: from bench towards bedside. *Oncotarget*. 2018;*9*(41):26507-26526.

56. Smit TH. The use of a quadruped as an in vivo model for the study of the spine - biomechanical considerations. *Eur Spine J*. 2002;11(2): 137-144.

SUPPORTING INFORMATION

Additional supporting information may be found online in the Supporting Information section at the end of this article.